The energy and temperature dependence of the electron-electron scattering rate in a one-dimensional surface superlattice

1998 J. Phys.: Condens. Matter 10 7793

(http://iopscience.iop.org/0953-8984/10/35/012)

J. Phys.: Condens. Matter **10** (1998) 7793–7808. Printed in the UK PII: S0953-8984(98)93624-4

The energy and temperature dependence of the electron–electron scattering rate in a one-dimensional surface superlattice

D Menashe† and B Laikhtman‡

Racah Institute of Physics, Hebrew University, Jerusalem 91904, Israel

Received 21 April 1998

Abstract. Increased interest in one-dimensional surface superlattices has motivated us to study the electron–electron scattering rate in these structures. Using a single-miniband model, we show a rich dependence of the scattering rate on the position of the Fermi level. This is particularly interesting from an experimental point of view, since the Fermi level can be externally controlled. When the Fermi level lies below the top of the miniband, the scattering rate is $\propto\Delta^2\ln(\epsilon_F/\Delta)$ (Δ is the temperature, or the electron's excess energy above the Fermi level, whichever is larger). This behaviour is similar to that of a uniform two-dimensional electron system. Near the top of the miniband, the Van Hove singularity in the energy spectrum strongly affects the scattering rate, which is $\propto\Delta$. Above the top of the miniband, the non-trivial shape of the Fermi surface leads to a rich dependence of the scattering rate on the wave vector of the scattered electron. This causes the scattering rate averaged over states near the Fermi surface to be $\propto\Delta^2\ln^2(\epsilon_F/\Delta)$. The method described here for calculating the scattering rate can be applied to any two-dimensional electron system with an arbitrary energy spectrum.

1. Introduction

In recent years there has been increased interest [1–6] in one-dimensional surface superlattices (1DSSLs), which are two-dimensional electron systems (2DESs) subjected to a one-dimensional periodic potential. Such systems are often realized by growing a periodic array of metallic wires on top of a quantum well heterostructure. By applying a voltage to these wires, one may induce a 1D periodic potential in the underlying 2DES, whose magnitude and form depend on the applied voltage. Using advanced fabrication techniques, it is possible to prepare samples with extremely high mobility (of the order of 10^7 cm^2 V^{-1} s^{-1} [7]), thus ensuring that effects due to the periodic potential can be observed experimentally. Adding to this the ability to independently control the electron concentration of the 2DES, and thus the Fermi energy, one can see that these systems are well suited for the study of various transport effects. Some examples are Wannier–Stark localization and Bloch oscillations [8], as well as novel magnetoresistance effects [4–6].

In this work we present a qualitative analysis of the electron–electron (e–e) scattering rate, τ_{e-e}^{-1}, in a 1DSSL. Besides being a key theoretical concept in interacting electron systems, in a 2DES the scattering rate also plays an important practical role in a number of physical processes, such as tunnelling [11], and dephasing of localized electrons [12, 13].

† E-mail: dmenashe@vms.huji.ac.il.
‡ E-mail: boris@vms.huji.ac.il.

0953-8984/98/357793+16$19.50

Furthermore, in a recent experiment Messica *et al* [1] reported a suppression of conductance by temperature and electric field in a 1DSSL. This effect was attributed to e–e scattering and is due to the non-trivial single-electron energy spectrum of the system. It is not observed in systems where the energy spectrum is quadratic (such as an n-type uniform GaAs/GaAlAs quantum well). One may define a measure of the contribution of e–e scattering to the resistivity in the form

$$\alpha \equiv \frac{ne^2}{m}\frac{\rho_{\mathrm{e-e}}}{\tau_{\mathrm{e-e}}^{-1}} \tag{1}$$

where n is the electron concentration and $\tau_{\mathrm{e-e}}^{-1}$ is the averaged scattering rate of all electrons within k_BT of the Fermi surface. α ($\lesssim 1$) describes the effectiveness of converting e–e scattering into resistivity. For a quadratic spectrum, $\alpha \equiv 0$, whereas $\alpha \sim 1$ for systems where the electron spectrum is markedly non-quadratic. This was nicely illustrated in the above-mentioned experiment, where α was observed to increase with the strength of the applied periodic potential. In the light of this, the results presented in this work regarding the e–e scattering rate are expected to be relevant to the conductance of a 1DSSL, even though this will not be discussed explicitly.

Another experiment in which one may expect to observe effects due to e–e scattering is one investigating the tunnelling between two quantum wells. In such an experiment one measures the I–V curve of the tunnelling current, which exhibits a resonance peak due to in-plane momentum conservation. Under certain conditions, e–e scattering is the dominant broadening mechanism for the resonance, thus providing a way to measure the e–e scattering rate. This method has already been used to measure the e–e scattering rate in a uniform 2DES [11]. Recently, a similar experiment involving tunnelling between a 2DES and a 1DSSL has been performed by Kardynal *et al* [3]. In this experiment the presence of many resonance peaks in the I–V curve was used to infer the existence of a miniband structure in the 1DSSL spectrum, as well as to model the form of the 1D periodic potential. While e–e scattering was not referred to in the above work, it may be possible in a future experiment to use the width of the resonances to measure various e–e scattering rates in a 1DSSL.

The main feature of a 1DSSL is the miniband structure of the energy spectrum. In this work we use a tight-binding model for the energy spectrum, and consider only a single occupied miniband. The scattering rate is studied using the Fermi golden rule together with an interaction potential whose exact form we do not specify. We show that these simplifications are justified if one is considering the analytic behaviour of the scattering rate, rather then exact numerical results. Despite the simplicity of the model, the behaviour of the e–e scattering rate has a rich dependence on the position of the Fermi level, which can be externally controlled in an experiment.

There are three energy scales relevant to the problem: ϵ_F, the Fermi energy; Λ, the miniband width; and Δ, which characterizes the excess energy of the test electron, or the temperature, whichever is larger. We show that if the Fermi level is below the top of the miniband, then the functional dependence of the e–e scattering rate on Δ is the same as that in a 2DES. However, when the Fermi level reaches the top of the miniband, the scattering rate is strongly enhanced due to the Van Hove singularity in the energy spectrum. Above the top of the miniband, the behaviour of the scattering rate depends strongly on the wave vector of the test electron. In general, this behaviour is similar to that when the Fermi level is below the top of the miniband, except near points on the Fermi surface with zero curvature, where the scattering rate is much larger. However, the zero-curvature points also have an effect on the *averaged* scattering rate, and cause it to be larger then when the Fermi level is below the top of the miniband.

One of the most interesting features of our model is the presence of a saddle point at the top of the miniband, which leads to the so-called Van Hove singularity in the density of states. The effect of a saddle point on the e–e scattering rate has been extensively studied within the context of high-T_c superconductivity [14–16]. However, it seems extremely difficult to experimentally separate out the effects of the saddle point from the other rich features present in high-T_c materials, such as nesting, and strong electron–electron correlations. On the other hand, in our model there is only one saddle point on the Fermi surface, no nesting, and no strong electron–electron correlations. This opens up the possibility of utilizing a 1DSSL to experimentally study the effect of a saddle point on the e–e scattering rate.

The rest of the paper is organized as follows. In section 2 we present the theoretical model used to calculate the e–e scattering rate. In section 3 we present a detailed analysis of the scattering rate, which enables us to identify the main qualitative features, as well as to obtain many exact results. In section 4 we concentrate on the effect of the Van Hove singularity on the e–e scattering rate, and in section 5 we discuss our results and summarize.

2. The theoretical model

In order to characterize the 1DSSL, we use the tight-binding approximation for the energy spectrum due to the 1D periodic potential [9]. Taking the x-direction to be the direction of the potential modulation, we write

$$\epsilon_{\boldsymbol{k}} = 2\Lambda - 2\Lambda \cos k_x a + \frac{\hbar^2 k_y^2}{2m} \tag{2}$$

where a is the period of the modulation, Λ is the overlap integral of the tight-binding Hamiltonian, and m is the effective mass. Also, we have added the constant 2Λ to the energy spectrum so that the bottom of the miniband corresponds to zero energy.

For energies below the top of the miniband, the iso-energy lines are closed, whereas above the top of the miniband, they are open. Exactly at the top of the miniband, the energy spectrum has a saddle point at $\boldsymbol{k} = (\pi/a, 0)$, which leads to the logarithmic Van Hove singularity in the density of states.

To calculate the e–e scattering rate we utilize the Fermi golden rule which we write as

$$\frac{1}{\tau_e(\boldsymbol{k})} = \frac{1}{4\pi^3\hbar} \int \mathrm{d}\epsilon_1 \ \mathrm{d}\epsilon_2 \ f(\epsilon_1 + \epsilon_2 - \epsilon_{\boldsymbol{k}})(1 - f(\epsilon_1))(1 - f(\epsilon_2)) I(\boldsymbol{k}, \epsilon_1, \epsilon_2) \tag{3}$$

where

$$I(\boldsymbol{k}, \epsilon_1, \epsilon_2) = \int \mathrm{d}\boldsymbol{k}_1 \ \mathrm{d}\boldsymbol{k}_2 \ |U(\boldsymbol{k} - \boldsymbol{k}_1)|^2 \delta(\epsilon_1 - \epsilon_{\boldsymbol{k}_1}) \delta(\epsilon_2 - \epsilon_{\boldsymbol{k}_2}) \times \delta(\epsilon_{\boldsymbol{k}_1} + \epsilon_{\boldsymbol{k}_2} - \epsilon_{\boldsymbol{k}} - \epsilon_{\boldsymbol{k}_1 + \boldsymbol{k}_2 - \boldsymbol{k}}). \tag{4}$$

$U(\boldsymbol{q})$ is the matrix element of the interaction potential,

$$f(\boldsymbol{k}) = f(\epsilon_{\boldsymbol{k}}) = [\mathrm{e}^{(\epsilon_{\boldsymbol{k}} - \epsilon_F)/k_B T} + 1]^{-1}$$

is the Fermi distribution function, and we have summed over the spin degrees of freedom. The quantity measured in many experiments, such as the tunnelling experiment described above and various interference experiments [17], is the energy relaxation rate, sometimes called the dephasing rate or the spectral broadening. It can be shown [18] that this quantity is directly related to the scattering rate calculated with the aid of the Fermi golden rule.

The calculations carried out in this work will be limited to the case where the scattered electron is near the Fermi surface and the temperature is much smaller than the Fermi energy. Defining the parameter

$$\Delta \equiv \max(|\epsilon_k - \epsilon_F|, k_B T)$$

one may write this condition as $\Delta \ll \epsilon_F$. Besides being relevant to most experiments, this is also the only case where one can examine the analytical behaviour of the Fermi golden rule.

Under the condition $\Delta \ll \epsilon_F$, it is possible to neglect dynamical screening effects and take the interaction potential between the electrons to be the statically screened Coulomb potential. In a uniform 2DES the matrix element for this potential is

$$U(\boldsymbol{q}) = 2\pi e^2/(\kappa(|\boldsymbol{q}| + q_s))$$

where κ is the background dielectric constant and $q_s = 2me^2/(\kappa\hbar^2)$. Assuming a GaAs/GaAlAs quantum well with a 2D electron concentration of $\sim 10^{11}$ cm^{-2}, it is easy to show that the Thomas–Fermi wave vector, q_s, is of the order of k_F, the Fermi wave vector. This means that the dependence of the matrix element on the transferred wave vector $\boldsymbol{q}$, is smooth on the scale of k_F. Under the condition $\Delta \ll \epsilon_F$, the transferred wave vector is less than, or of the order of, k_F, so $U(\boldsymbol{q})$ is smooth over the whole region of integration in the Fermi golden rule. In a 1DSSL the situation is more complicated, and to our knowledge a comprehensive description of the screening has yet to be given. Even with the single-miniband model that we use here, the analysis is quite complicated, and only approximate results have been derived for a few specific limits [10]. However, it seems reasonable to assume that the screened potential still has a smooth $\boldsymbol{q}$-dependence, and hence that the analytic behaviour of the scattering rate is unaffected by the exact form of $U(\boldsymbol{q})$ and is determined solely by phase-space considerations. Furthermore, we will show that only specific scattering processes, corresponding to specific values of the transferred wave vector, contribute to the leading-order term of the scattering rate. This enables us to give the scattering rate in terms of specific values of $U(\boldsymbol{q})$ without knowing the full functional form (a similar situation arises for the uniform 2DES [20]).

3. A detailed analysis of the scattering rate

We begin our analysis of the scattering rate by noting that in the limit $\Delta \ll \epsilon_F$, the presence of the Fermi functions limits the region of the energy integrations in equation (3) to within Δ of the Fermi energy. This means that the energies ϵ_1 and ϵ_2 appearing in $I(\boldsymbol{k}, \epsilon_1, \epsilon_2)$ are close to ϵ_F. We will show that for a 2D system $I(\boldsymbol{k}, \epsilon_1, \epsilon_2)$ always diverges in the limit $\Delta \to 0$, with the divergence being mostly logarithmic, but sometimes of higher order. The logarithmic divergence has long been known of for the special case of a uniform 2DES [21, 22], whereas certain aspects of the general 2D system have been studied by Fukuyama and Ogata [23]. The divergence of $I(\boldsymbol{k}, \epsilon_1, \epsilon_2)$ as $\Delta \to 0$ means that the main contribution to it comes from specific regions of the 4D $\boldsymbol{k}_1$–$\boldsymbol{k}_2$ space. This in turn means that the dominant contribution to the scattering rate comes from specific scattering process, and not all scattering processes allowed by momentum and energy conservation laws.

In appendix A we show that for a scattering process to be dominant, $\boldsymbol{k}_1$ and $\boldsymbol{k}_2$ must be close to the vectors $\boldsymbol{k}_1^0$ and $\boldsymbol{k}_2^0$ respectively, such that one of the following conditions is satisfied:

$$\boldsymbol{v}_{\boldsymbol{k}_1^0} = 0 \qquad \text{or} \qquad \boldsymbol{v}_{\boldsymbol{k}_2^0} = 0 \qquad \text{or} \qquad \boldsymbol{v}_{\boldsymbol{k}_1^0 + \boldsymbol{k}_2^0 - \boldsymbol{k}} = 0 \tag{5a}$$

$$\boldsymbol{v}_{\boldsymbol{k}_1^0} \parallel \boldsymbol{v}_{\boldsymbol{k}_2^0} \parallel \boldsymbol{v}_{\boldsymbol{k}_1^0 + \boldsymbol{k}_2^0 - \boldsymbol{k}} \tag{5b}$$

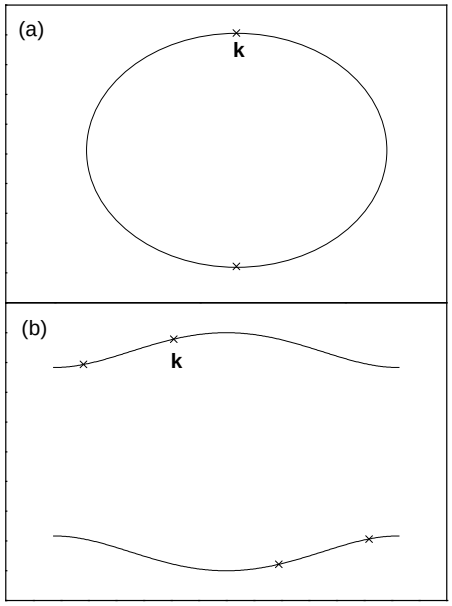

Figure 1. Points on the Fermi surface which have velocity parallel to that of a given wave vector $\boldsymbol{k}$. (a) For a closed and convex Fermi surface there is only one such point (at $-\boldsymbol{k}$). (b) For an open Fermi surface, like that occurring when the Fermi level is above the top of the miniband, there are three such points (except when $\boldsymbol{k}$ is at a zero-curvature point, where the four points displayed merge into two).

where $\boldsymbol{v}_{\boldsymbol{q}}$ is the velocity corresponding to wave vector $\boldsymbol{q}$. An additional implicit condition is of course that $\boldsymbol{k}_1^0$ and $\boldsymbol{k}_2^0$ describe a legitimate scattering process, i.e. that all of the vectors $\boldsymbol{k}_1^0$, $\boldsymbol{k}_2^0$, and $\boldsymbol{k}_1^0 + \boldsymbol{k}_2^0 - \boldsymbol{k}$ are within energy distance Δ of the Fermi surface.

Condition (5*a*) means that the corresponding wave vector, $\boldsymbol{k}_1^0$, $\boldsymbol{k}_2^0$, or $\boldsymbol{k}_1^0 + \boldsymbol{k}_2^0 - \boldsymbol{k}$, is at a saddle point, and this can only occur if the Fermi surface is within the energy distance Δ of such a point. On the other hand, condition (5*b*), which means that the energy surface is parallel at the three points $\boldsymbol{k}_1^0$, $\boldsymbol{k}_2^0$, and $\boldsymbol{k}_1^0 + \boldsymbol{k}_2^0 - \boldsymbol{k}$, is much more general and can be satisfied for any Fermi surface. In fact, due to the time-reversal symmetry, $\epsilon_{\boldsymbol{k}} = \epsilon_{-\boldsymbol{k}}$, it is easy to see that there are three different scattering processes which always satisfy this condition. These are

$$\boldsymbol{k}_1^0 = \boldsymbol{k}_2^0 = \boldsymbol{k} \tag{6a}$$

$$\boldsymbol{k}_1^0 = -\boldsymbol{k}_2^0 = \boldsymbol{k} \tag{6b}$$

$$-\boldsymbol{k}_1^0 = \boldsymbol{k}_2^0 = \boldsymbol{k}. \tag{6c}$$

For a non-nested and convex Fermi surface, these are the only possible processes that satisfy condition (5*b*) (see figure 1(a)), whereas we shall see that for a more complex Fermi surface, other processes may also be possible.

Up till now, all that has been said refers to a general 2DES, the only limitation being that $\Delta \ll \epsilon_F$. We shall now apply the above results to the model under discussion, and identify the dominant scattering processes. Following this we will calculate the contribution of these processes to the scattering rate.

As was discussed in the introduction, we distinguish between three different regimes of our model.

(i) *First regime.* When the Fermi level is below the top of the miniband, $\epsilon_F < 4\Lambda$ and $|\epsilon_F - 4\Lambda| \gg \Delta$, then the Fermi surface is closed and convex. This means that the only dominant scattering processes are those described by equations (6). The contribution of these scattering processes is calculated with the aid of appendix B. For the contribution of the scattering process corresponding to equation (6*a*) we obtain

$$I^a(\boldsymbol{k}, \epsilon_1, \epsilon_2) = \frac{m|U(0)|^2}{\hbar^2 a^2 \Lambda |\alpha(\boldsymbol{k})|}\left[\ln\frac{\pi|\alpha(\boldsymbol{k})|}{|\epsilon_1 - \epsilon_{\boldsymbol{k}}|} + \ln\frac{\pi|\alpha(\boldsymbol{k})|}{|\epsilon_2 - \epsilon_{\boldsymbol{k}}|}\right] \tag{7}$$

where $\alpha(\boldsymbol{k})$ is proportional to the curvature of the energy surface at $\boldsymbol{k}$ and is given by

$$\alpha(\boldsymbol{k}) = 2\Lambda \sin^2(k_x a) + \frac{\hbar^2 k_y^2}{m}\cos(k_x a). \tag{8}$$

The above result is valid as long as $\alpha(\boldsymbol{k})$ is not small (the lower limit is set by equation (B9)), which in effect means that the curvature of the Fermi surface near the point $\boldsymbol{k}$ is non-zero. This is always true for the first regime, since the Fermi surface is closed and convex. In fact, it can be seen from the definition of $\alpha(\boldsymbol{k})$ that it is generally of the order of ϵ_F.

The contributions of scattering processes (6*b*) and (6*c*) to $I(\boldsymbol{k}, \epsilon_1, \epsilon_2)$ can be calculated using exactly the same method as is presented in appendix B. The results are also identical except for the process corresponding to equation (6*c*), where the matrix element $U(0)$ is replaced by $U(2\boldsymbol{k})$. Since the total value of $I(\boldsymbol{k}, \epsilon_1, \epsilon_2)$ is just the sum of the contributions from the three dominant scattering processes, we see that

$$I(\boldsymbol{k}, \epsilon_1, \epsilon_2) = 2I^a(\boldsymbol{k}, \epsilon_1, \epsilon_2) + (U^2(2\boldsymbol{k})/U^2(0))I^a(\boldsymbol{k}, \epsilon_1, \epsilon_2).$$

Inserting this into equation (3), and using the working assumption that $\Delta \ll \epsilon_F$ and $\alpha(\boldsymbol{k}) \sim \epsilon_F$, it is clear that the scattering rate is of the order of $\Delta^2 \ln(\epsilon_F/\Delta)$. Thus we see that for the first regime the scattering rate has the same functional form as that of the uniform 2DES. The integral can be calculated exactly for the two limiting cases $\epsilon_F \gg |\epsilon_{\boldsymbol{k}} - \epsilon_F| \gg k_B T$ and $\epsilon_F \gg k_B T \gg |\epsilon_{\boldsymbol{k}} - \epsilon_F|$, where we obtain

$$\frac{1}{\tau_e(\boldsymbol{k})} = \begin{cases} \dfrac{m(2|U(0)|^2 + |U(2\boldsymbol{k})|^2)}{8\pi\hbar^3 a^2 \Lambda |\alpha(\boldsymbol{k})|}(k_B T)^2 & \\ \quad \times \ln\left[\dfrac{\epsilon_F}{k_B T}\right] & \text{for } \epsilon_F \gg k_B T \gg |\epsilon_{\boldsymbol{k}} - \epsilon_F| \\ \dfrac{m(2|U(0)|^2 + 2|U(2\boldsymbol{k})|^2)}{4\pi^3\hbar^3 a^2 \Lambda |\alpha(\boldsymbol{k})|}|\epsilon_{\boldsymbol{k}} - \epsilon_F|^2 & \\ \quad \times \ln\left[\dfrac{\epsilon_F}{|\epsilon_{\boldsymbol{k}} - \epsilon_F|}\right] & \text{for } \epsilon_F \gg |\epsilon_{\boldsymbol{k}} - \epsilon_F| \gg k_B T. \end{cases} \tag{9}$$

(ii) *Second regime.* If the Fermi surface is near the top of the miniband, $|\epsilon_F - 4\Lambda| \lesssim \Delta$, then the saddle point in the energy spectrum comes into play and has a strong effect on the scattering rate. This can be seen formally from the fact that condition (5*a*) can be satisfied when the Fermi level is near the top of the miniband, whereas in the general case it cannot. The details of the scattering rate for this regime will be handled separately in section 4.

(iii) *Third regime.* When the Fermi level is above the top of the miniband, $\epsilon_F > 4\Lambda$ and $|\epsilon_F - 4\Lambda| \gg \Delta$, the Fermi surface is open and concave. The main consequence of this is that there are points on the Fermi surface which have zero curvature, and for electrons near these points the scattering rate is markedly different to that for the rest of the Fermi surface.

For electrons not in the vicinity of one of the zero-curvature points (the exact criteria are defined in equation (B9)), the contribution of the three processes of equations (6) to the

scattering rate can be dealt with in the same manner as for the first regime. This means that equation (7) describes the contribution of process (6*a*) to $I(\boldsymbol{k}, \epsilon_1, \epsilon_2)$ and equation (9) describes the total contribution of the three processes to the scattering rate. However, contrary to the case for the first regime, there are other processes that contribute to the scattering rate, besides the above-mentioned three. The reason for this is that for a given wave vector, $\boldsymbol{k}$, there are three different points on the Fermi surface whose velocity is parallel to $\boldsymbol{v}_{\boldsymbol{k}}$ (figure 1(b)), as opposed to one when the Fermi surface is closed and convex (figure 1(a)). These extra points on the Fermi surface mean that there are eight more dominant scattering processes besides the three original ones. Due to the non-trivial nature of the energy spectrum, these extra processes are more onerous to analyse, and their exact contribution to the scattering rate will not be given here. Instead, at the end of appendix B we show that they make a similar contribution to the scattering rate to the original three. Thus we must keep in mind that the actual scattering rate for this regime is two to three times larger than that given by equation (9), which includes just the three original processes.

For electrons near the zero-curvature points, the contribution of process (6*a*) to $I(\boldsymbol{k}, \epsilon_1, \epsilon_2)$ is calculated in appendix B, and is given by

$$I^a(\boldsymbol{k}, \epsilon_1, \epsilon_2) = \frac{m^{3/2}|U(0)|^2}{4\hbar^3 a^2 \Lambda^{3/2}|k_y \sin k_x a|} \times \left[\frac{2}{|\epsilon_{\boldsymbol{k}} - \epsilon_1|^2 + |\epsilon_{\boldsymbol{k}} - \epsilon_2|^2}\right]^{1/4} \eta\left[\frac{2\epsilon_{\boldsymbol{k}} - \epsilon_1 - \epsilon_2}{\sqrt{2|\epsilon_{\boldsymbol{k}} - \epsilon_1|^2 + 2|\epsilon_{\boldsymbol{k}} - \epsilon_2|^2}}\right] \tag{10}$$

where

$$\eta(x) = \frac{4}{\sqrt{1+x}} F\left[\frac{\arccos(-x)}{2}, \frac{2}{1+x}\right]$$

and

$$F(\phi, a) \equiv \int_0^{\phi} (1 - a\sin^2\theta)^{-1/2}\, \mathrm{d}\theta$$

is the elliptic integral of the first kind. Note that the limit $k_y \to 0$ does not present a problem as regards the above result, as this limit means that k is near the saddle point, and is treated separately in section 4. Similarly, the limit $\sin(k_x a) \to 0$ is also irrelevant since it is easy to see that if $\alpha(\boldsymbol{k})$ is small, and we are not near the saddle point, then $\sin(k_x a)$ cannot be small.

As before, the contributions of the other scattering processes (equations (6*b*) and (6*c*)) are identical except for the different matrix element, so

$$I(\boldsymbol{k}, \epsilon_1, \epsilon_2) = 2I^a(\boldsymbol{k}, \epsilon_1, \epsilon_2) + (U^2(2\boldsymbol{k})/U^2(0))I^a(\boldsymbol{k}, \epsilon_1, \epsilon_2).$$

Inserting this into the expression for the scattering rate, it is easy to see that the final result is proportional to $\Delta^{3/2}$, as compared to $\Delta^2 \ln(\epsilon_F/\Delta)$ when the curvature is non-zero. For the two limiting cases $\epsilon_F \gg |\epsilon_{\boldsymbol{k}} - \epsilon_F| \gg k_B T$ and $\epsilon_F \gg k_B T \gg |\epsilon_{\boldsymbol{k}} - \epsilon_F|$, we can scale the integral and perform the resulting dimensionless integral numerically, thus obtaining

$$\frac{1}{\tau_e(\boldsymbol{k})} = \begin{cases} \dfrac{4.86m^{3/2}(2|U(0)|^2 + |U(2\boldsymbol{k})|^2)}{16\pi\hbar^4 a^2 \Lambda^{3/2}|k_y \sin k_x a|}(k_B T)^{3/2} & \text{for } \epsilon_F \gg k_B T \gg |\epsilon_{\boldsymbol{k}} - \epsilon_F| \\ \dfrac{6.61m^{3/2}(2|U(0)|^2 + |U(2\boldsymbol{k})|^2)}{16\pi\hbar^4 a^2 \Lambda^{3/2}|k_y \sin k_x a|}|\epsilon_{\boldsymbol{k}} - \epsilon_F|^{3/2} & \text{for } \epsilon_F \gg |\epsilon_{\boldsymbol{k}} - \epsilon_F| \gg k_B T. \end{cases} \tag{11}$$

Note that even though the above result only accounts for the three scattering processes of equations (6), it is exact for the case in which $\boldsymbol{k}$ is near a zero-curvature point. The reason for this is that in this case there is only one other point on the Fermi surface whose velocity is parallel to $\boldsymbol{v}_{\boldsymbol{k}}$, as opposed to three points in the non-zero-curvature case (figure 1(b)).

4. Near the Van Hove singularity

In this section we deal with the case where the Fermi energy is near the saddle point in the energy spectrum. Since the saddle point is at the top of the miniband, this means that

$$|\epsilon_F - 4\Lambda| \lesssim \Delta. \tag{12}$$

In order to derive an analytic expression for the scattering rate, it is necessary to assume a stronger inequality, specifically $|\epsilon_F - 4\Lambda| \ll \Delta$. We shall only refer to the general case at the end of this section, whereas until then we will indeed assume the stronger inequality (which in effect means that the Fermi level is exactly at the saddle point).

As we noted in the introduction, the general case of a saddle point in the energy spectrum has been studied within the context of high-T_c superconductivity [14–16]. It has been shown that the behaviour of the scattering rate $\tau_{\mathrm{e}}^{-1}(\boldsymbol{k})$ depends strongly on $\boldsymbol{k}$, the wave vector of the scattered electron. For $\boldsymbol{k}$ near the saddle point, the scattering rate is proportional to Δ, whereas for $\boldsymbol{k}$ far away from the saddle point, the scattering rate is proportional to $\Delta^{3/2}$. Since the main contribution to the logarithmically large density of states comes from values of $\boldsymbol{k}$ near the saddle point, we will focus on this case in the present work. For the case in which $\boldsymbol{k}$ is far away from the saddle point, the reader is referred to Gopalan *et al* [14].

Due to the special nature of the energy spectrum at the saddle point, the general analysis of the scattering rate carried out in the previous section cannot be applied here. Specifically, instead of trying to calculate the function $I(\boldsymbol{k}, \epsilon_1, \epsilon_2)$, and the performing the energy integral in equation (3), we first perform the trivial energy integrals so that we are left with the momentum integrals. As we shall soon see, the main contribution to these integrals comes from the region where $\boldsymbol{k}_1$ and $\boldsymbol{k}_2$ are near the saddle point, and since $\boldsymbol{k}$ is also near the saddle point, this means that $\boldsymbol{k}_1 + \boldsymbol{k}_2 - \boldsymbol{k}$ is near the saddle point as well. The fact that the main contribution to the scattering rate comes from scattering processes where all four electrons are near the saddle point enables us to expand all of the energies in equation (3) around this point. The expansion of ϵ_k around the wave vector $(\pi/a, 0)$ leads to the result

$$\epsilon_{\boldsymbol{k}} = 4\Lambda - \Lambda xy \tag{13}$$

where

$$x = (k_x a - \pi) + \hbar k_y/\sqrt{2m\Lambda} \qquad \text{and} \qquad y = (k_x a - \pi) - \hbar k_y/\sqrt{2m\Lambda}.$$

Using the same expansion for all of the energies in equation (3), and rescaling the integral accordingly, one obtains

$$\begin{aligned}\frac{1}{\tau_{\mathrm{e}}(\boldsymbol{k})} = \frac{m\Lambda|U(0)|^2}{2\pi^3\hbar^3 a^2}\int_{-\infty}^{\infty} \mathrm{d}x_1\ \mathrm{d}y_1\ \mathrm{d}x_2\ \mathrm{d}y_2\ f(4\Lambda - \Lambda(x_1y_1 + x_2y_2 - xy)) \\ \times\ (1 - f(4\Lambda - \Lambda x_1y_1))(1 - f(4\Lambda - \Lambda x_2y_2)) \\ \times\ \delta(\Lambda(xy_1 + yx_1 + xy_2 + yx_2 - x_1y_2 - x_2y_1 - 2xy))\end{aligned} \tag{14}$$

where the limits of integration have been taken to infinity in view of the assumption that the main contribution to the integral comes from small x_i and y_i.

The integral in equation (14) can be solved for the two limiting cases

$$\epsilon_F \gg |\epsilon_{\boldsymbol{k}} - \epsilon_F| \gg k_B T \qquad \text{and} \qquad \epsilon_F \gg k_B T \gg |\epsilon_{\boldsymbol{k}} - \epsilon_F|.$$

The first case has been dealt with by Gopalan *et al* [14], whereas the second case, to our knowledge, has yet to be dealt with. For the first case we obtain

$$\frac{1}{\tau_e(\boldsymbol{k})} = \frac{4m|U(0)|^2|\epsilon_{\boldsymbol{k}} - \epsilon_F|}{\pi^3\hbar^3 a^2\Lambda} \tag{15}$$

where it is easily seen that the main contribution to the integral in equation (14) comes from the region where $x_i \approx x$ and $y_i \approx y$ ($i = 1, 2$). This in turn means that our original assumption (that the main contribution to the scattering rate comes from scattering processes where all four electrons are near the saddle point), is indeed correct.

As for the second case, one may make the transformations $x_i \to x_i$ and $\Lambda x_i y_i \to \epsilon_i$ ($i = 1, 2$), so that equation (14) becomes

$$\begin{aligned}\frac{1}{\tau_e(\boldsymbol{k})} = {} & \frac{m|U(0)|^2}{2\pi^3\hbar^3 a^2\Lambda}\int_{-\infty}^{\infty} \mathrm{d}\epsilon_1\ \mathrm{d}\epsilon_2\ f(4\Lambda - \epsilon_1 - \epsilon_2)(1 - f(4\Lambda - \epsilon_1))(1 - f(4\Lambda - \epsilon_2)) \\ & \times \int_{-\infty}^{\infty} \mathrm{d}x_1\ \mathrm{d}x_2\ \delta(\Lambda y(x_1^2 x_2 + x_2^2 x_1) + x(\epsilon_2 x_1 + \epsilon_1 x_2) - \epsilon_2 x_1^2 - \epsilon_1 x_2^2). \end{aligned} \tag{16}$$

In the above integral we have neglected the term proportional to $\Lambda xy = \epsilon_{\boldsymbol{k}} - \epsilon_F$, since according to our present assumption, it is small compared to ϵ_1 and ϵ_2 (which are $\sim k_B T$). By the same reasoning we can assume that $x \ll x_i$ and $y \ll \epsilon_i/x_i$, and hence that the dominant terms in the δ-function are the two quadratic terms. This means that only the regions where $\epsilon_1\epsilon_2 < 0$ contribute to the integral, and also that

$$|x_2| \approx \sqrt{|\epsilon_2/\epsilon_1|}|x_1|.$$

Therefore, if we define

$$g_\pm(x_1) \equiv \Lambda y(x_1^3|\epsilon_2/\epsilon_1| \pm |x_1^3|\sqrt{|\epsilon_2/\epsilon_1|}) + x\epsilon_2(x_1 \mp \sqrt{|\epsilon_1/\epsilon_2|}|x_1|)$$

(where the $\pm$ sign corresponds to $x_2 \approx \pm\sqrt{|\epsilon_2/\epsilon_1|}|x_1|$), we may write

$$\begin{aligned}\frac{1}{\tau_e(\boldsymbol{k})} = {} & \frac{m|U(0)|^2}{\pi^3\hbar^3 a^2\Lambda}\int_{-\infty}^{\infty} \mathrm{d}\epsilon_1\ \mathrm{d}\epsilon_2\ f(4\Lambda - \epsilon_1 - \epsilon_2)(1 - f(4\Lambda - \epsilon_1))(1 - f(4\Lambda - \epsilon_2)) \\ & \times \Theta(\epsilon_1)\Theta(-\epsilon_2)\int_{-\infty}^{\infty} \mathrm{d}x_1\ \mathrm{d}x_2\ \delta(g_\pm(x_1) - \epsilon_2 x_1^2 - \epsilon_1 x_2^2) \\ = {} & \frac{m|U(0)|^2}{\pi^3\hbar^3 a^2\Lambda}\int_{-\infty}^{\infty} \mathrm{d}\epsilon_1\ \mathrm{d}\epsilon_2\ f(4\Lambda - \epsilon_1 - \epsilon_2)(1 - f(4\Lambda - \epsilon_1))(1 - f(4\Lambda - \epsilon_2)) \\ & \times \frac{\Theta(\epsilon_1)\Theta(-\epsilon_2)}{\sqrt{|\epsilon_1\epsilon_2|}}\int_{-\infty}^{\infty} \mathrm{d}x_1 \left[\frac{1}{2\sqrt{x_1^2 - g_+(x_1)/\epsilon_2}} + \frac{1}{2\sqrt{x_1^2 - g_-(x_1)/\epsilon_2}}\right]. \end{aligned} \tag{17}$$

Without the small correction $g_\pm(x_1)/\epsilon_2$ in the square root, the x_1-integral would diverge logarithmically at zero and infinity. However, the linear term in g cuts off the divergence at zero, whereas the cubic term cuts off the divergence at infinity, so

$$\begin{aligned}\frac{1}{\tau_e(\boldsymbol{k})} = {} & \frac{2m|U(0)|^2}{\pi^3\hbar^3 a^2\Lambda}\int_{-\infty}^{\infty} \mathrm{d}\epsilon_1\ \mathrm{d}\epsilon_2\ f(4\Lambda - \epsilon_1 - \epsilon_2)(1 - f(4\Lambda - \epsilon_1))(1 - f(4\Lambda - \epsilon_2)) \\ & \times \frac{\Theta(\epsilon_1)\Theta(-\epsilon_2)}{\sqrt{|\epsilon_1\epsilon_2|}} \ln\left|\frac{\epsilon_2}{\epsilon_{\boldsymbol{k}} - \epsilon_F}\right| \end{aligned} \tag{18}$$

where we have neglected factors of order unity within the logarithm. The remaining energy integrals may be scaled with respect to k_BT and the resulting dimensionless integrals solved numerically, thus leading to the final result

$$\frac{1}{\tau_e(\boldsymbol{k})} = \frac{2.14m|U(0)|^2 k_BT}{\pi^3\hbar^3 a^2\Lambda} \ln\left|\frac{k_BT}{\epsilon_{\boldsymbol{k}} - \epsilon_F}\right|. \tag{19}$$

To end this section, we shall discuss briefly what happens when the condition $|\epsilon_F - 4\Lambda| \ll \Delta$ is relaxed and only equation (12) is valid. Gopalan *et al* [14] have studied this case numerically, and their results seem to indicate that $\tau_e^{-1}(\boldsymbol{k}) \propto \Delta^\zeta$ where $1 < \zeta < 2$. In the limit where $|\epsilon_F - 4\Lambda| \ll \Delta$, which we have just studied, $\zeta \to 1$. In the opposite limit, $|\epsilon_F - 4\Lambda| \gg \Delta$, the scattered electron does not feel the effect of the saddle point, so $\zeta \to 2$, just as in the usual 2D case. In between these two limits, the value of the exponent ζ was observed to change smoothly between 1 and 2.

5. Discussion and summary

In sections 3 and 4 we have presented a detailed analysis of $\tau_e^{-1}(\boldsymbol{k})$, the scattering rate for an electron in state $|\boldsymbol{k}\rangle$. The purpose of this analysis is to determine the analytic behaviour of the scattering rate for different regimes of our model, rather then to derive exact numerical results. The main assumption made was that $\Delta \ll \epsilon_F$, where $\Delta \equiv \max(|\epsilon_{\boldsymbol{k}} - \epsilon_F|, k_BT)$. This assumption allowed us to identify specific scattering processes which make the dominant contribution to the scattering rate, and also to calculate this contribution. We note that the method developed here is quite general in nature and can be applied to any 2DES with an arbitrary energy spectrum.

In many experiments one is often interested in the scattering rate averaged over the Fermi surface, and not the scattering rate for a specific wave vector $\boldsymbol{k}$. In a 2DES with an isotropic energy spectrum, these two quantities are identical, whereas in our model, which has a strongly anisotropic energy spectrum (equation (2)), there can be a marked $\boldsymbol{k}$-dependence of the scattering rate. The exact nature of the averaging depends on the type of experiment being performed, but generally has the form

$$\frac{1}{\tau_{e-e}(T)} = \left(\int d\boldsymbol{k}\ \tau_{e-e}^{-1}(\boldsymbol{k}) W(\epsilon_k)\right) \Big/ \left(\int d\boldsymbol{k}\ W(\epsilon_k)\right) \tag{20}$$

where the function $W(\epsilon_k)$ determines the relative importance of the different states near the Fermi surface. In a tunnelling experiment performed at finite temperature, one would take $W(\epsilon) = (df/d\epsilon)_{\epsilon=\epsilon_F}$ so that states within k_BT of the Fermi surface take part in the averaging. If the voltage bias, V, is large compared to the temperature, then the averaging must be taken over all states with energy $\epsilon_F + eV$, and hence $W(\epsilon) = \delta(\epsilon_F + eV - \epsilon)$. This type of averaging can also be relevant to interference experiments [17] and magnetic focusing experiments [19] performed at low temperature. Due to the fact that the matrix element of the screened Coulomb interaction is not calculated (see the discussion at the end of section 1), we can only give order-of-magnitude estimates for the averaged scattering rate, which will now be discussed.

The three different regimes of our model are characterized by the position of the Fermi level relative to the top of the miniband. If the Fermi level is below the top of the miniband, then only the three scattering processes of equations (6) make a dominant contribution to the scattering rate, which is given by equation (9). This result is similar to that for the uniform 2DES case, the main difference being the strong $\boldsymbol{k}$-dependence of the scattering

rate. The averaged scattering rate for this case is given by

$$\frac{1}{\tau_{av}(\Delta)} \approx \frac{m|U(0)|^2\Delta^2}{\hbar^3 a^2 \Lambda \epsilon_F} \ln\left[\frac{\epsilon_F}{\Delta}\right]. \tag{21}$$

When the Fermi level is near the top of the miniband, then the saddle point in the energy spectrum has a strong effect on the scattering rate. For $\boldsymbol{k}$ near the saddle point, and for $|\epsilon_{\boldsymbol{k}} - \epsilon_F| \gg k_B T, |\epsilon_F - 4\Lambda|$, the scattering rate is given by equation (15). If, on the other hand, $k_B T \gg |\epsilon_{\boldsymbol{k}} - \epsilon_F|, |\epsilon_F - 4\Lambda|$, the scattering rate is given by equation (19). Taken together, these two equations mean that as long as $\Delta \gg |\epsilon_F - 4\Lambda|$ and $\boldsymbol{k}$ is near the saddle point, then $\tau_e^{-1}(\boldsymbol{k}) \propto \Delta$. If $\boldsymbol{k}$ is not near the saddle point but $\Delta \gg |\epsilon_F - 4\Lambda|$ still holds true, then Gopalan *et al* [14] have shown that $\tau_e^{-1}(\boldsymbol{k}) \propto \Delta^{3/2}$. However, states far away from the saddle point contribute much less to the logarithmically large density of states, so the states near the saddle determine the averaged scattering rate, which is

$$\frac{1}{\tau_{av}(\Delta)} \approx \frac{m|U(0)|^2\Delta}{\hbar^3 a^2 \Lambda}. \tag{22}$$

Note that the logarithmic factor in equation (19) does not appear in the averaged scattering rate, since for $T > 0$ one must average over all states within $k_B T$ of the Fermi energy.

In the last regime, where the Fermi level is above the top of the miniband, we distinguish between two cases. If $\boldsymbol{k}$ is not near a point on the Fermi surface with zero curvature, then the behaviour of the scattering rate is similar to that of the first regime. However, due to the non-trivial shape of the Fermi surface, other scattering processes, besides the three described in equations (6), make a contribution to the scattering rate. This means that equation (9), which includes only contributions from the three above-mentioned processes, is only correct to within an order of magnitude, and the proper result should be two to three times larger; if $\boldsymbol{k}$ is near a zero-curvature point on the Fermi surface then the scattering rate is markedly different from the usual 2D case, and is given by equation (11). While the scattering rate near zero-curvature points is much larger then the scattering rate near other points on the Fermi surface, these points do not have a direct qualitative effect on the averaged scattering rate. The reason for this is that equation (11) is valid only for small portions of the Fermi surface around the zero-curvature points. Since the length of these portions is $\propto\Delta^{1/2}$ (equation (B9)), and since the scattering rate there is of the order of $\Delta^{3/2}$, the total contribution to the averaged scattering rate is only $\propto\Delta^2$, which is not larger than the total contribution of other points on the Fermi surface. However, the zero-curvature points do have an indirect effect on the averaged scattering rate in that equation (11) diverges as $1/x$, where x is the distance along the Fermi surface from the nearest saddle point. The averaged scattering rate is thus

$$\frac{1}{\tau_{av}(\Delta)} \approx \frac{m|U(0)|^2}{\hbar^3 a^2 \Lambda \epsilon_F} \ln^2\left[\frac{\epsilon_F}{\Delta}\right] \tag{23}$$

which is larger than the usual 2D result by an extra logarithmic factor.

As we noted in section 1, all of the results presented in this work refer to a single-miniband model of a 1DSSL. Since a typical sample will have more than one occupied miniband, we now discuss briefly the possible effect of the multiplicity of minibands on the scattering rate. For an electron in a given miniband, the presence of other minibands means that inter-miniband scattering may take place as well as intra-miniband scattering. This in turn means that the total scattering rate is enhanced compared to the intra-miniband scattering rate. However, we argue that this enhancement is only of the order of the number of occupied minibands, and is not qualitative in nature. The reason for this is that the presence of other minibands only means that the Fermi surface has other disconnected

sections, besides the section belonging to the given miniband. Following the analysis in section 3, it should be clear that these additional sections of the Fermi surface give rise to additional dominant scattering processes, whose contribution to the scattering rate is similar to the contribution of the scattering processes described by equations (6). A possible exception to this argument arises when the Fermi level is such that it lies near the top of one of the minibands. In that case the rate of scattering of an electron in our given miniband will be dominated by processes involving the saddle point of the other miniband. The scattering rate in this case will be similar to the intra-miniband scattering rate for an electron lying in the same miniband as the saddle point, but far away from it, i.e. $\propto\Delta^{3/2}$.

In conclusion, we have studied theoretically the scattering rate due to e–e scattering in a 1DSSL. On the basis of our results for a single-miniband model, we conclude that the scattering rate exhibits various types of functional dependence on the temperature and the energy of the scattered electron. In the introduction, we discussed possible experiments which are affected by e–e scattering, and in which the full range of this behaviour should be observable by controlling the position of the Fermi level. We hope that the results presented in this work will motivate further theoretical and experimental research into this subject.

Acknowledgments

We are grateful to Y Naveh for reading the manuscript and for making useful comments. This research was supported by The S A Schonbrunn Research Endowment Fund.

Appendix A. Identification of dominant scattering processes

In this appendix we derive the necessary conditions for a scattering process to make a dominant contribution to the scattering rate. The exact contribution of each of these processes, and whether they are in fact dominant, is studied in sections 3 and 4.

From the discussion at the beginning of section 3, it is clear that to identify the dominant scattering processes, one must identify the regions of the 4D $\boldsymbol{k}_1$–$\boldsymbol{k}_2$ space which make divergent contributions to the function $I(\boldsymbol{k},\epsilon_1,\epsilon_2)$ (defined in equation (4)) in the limit $\Delta\to 0$. To do this, let us imagine a scattering process in which the vectors $\boldsymbol{k}_1$ and $\boldsymbol{k}_2$ are close to vectors $\boldsymbol{k}_1^0$ and $\boldsymbol{k}_2^0$ respectively, and expand the integrand in equation (4) in the small variables $\boldsymbol{r}_i=\boldsymbol{k}_i-\boldsymbol{k}_i^0$, thus obtaining

$$I(\boldsymbol{k},\epsilon_1,\epsilon_2)=\int \mathrm{d}\boldsymbol{r}_1\ \mathrm{d}\boldsymbol{r}_2\ |U(\boldsymbol{k}-\boldsymbol{k}_1^0-\boldsymbol{r}_1)|^2\delta(\omega_1-\boldsymbol{v}_1\boldsymbol{r}_1)\delta(\omega_2-\boldsymbol{v}_2\boldsymbol{r}_2)\times\delta(\epsilon-\boldsymbol{v}(\boldsymbol{r}_1+\boldsymbol{r}_2)). \tag{A1}$$

In the above integral $\boldsymbol{v}_{\boldsymbol{q}}\equiv\partial\epsilon_{\boldsymbol{q}}/\partial\boldsymbol{q}$ is the velocity at the point $\boldsymbol{q}$, and we have defined the following quantities:

$$\begin{aligned}
&\omega_i\equiv\epsilon_i-\epsilon_{\boldsymbol{k}_i^0}\qquad(i=1,2)\\
&\boldsymbol{v}_i\equiv\boldsymbol{v}_{\boldsymbol{k}_i^0}\qquad(i=1,2)\\
&\epsilon\equiv\epsilon_1+\epsilon_2-\epsilon_{\boldsymbol{k}}-\epsilon_{\boldsymbol{k}_1^0+\boldsymbol{k}_2^0-\boldsymbol{k}}\\
&\boldsymbol{v}\equiv\boldsymbol{v}_{\boldsymbol{k}_1^0+\boldsymbol{k}_2^0-\boldsymbol{k}}.
\end{aligned}$$

Since we are assuming that the matrix element $U(\boldsymbol{q})$ depends smoothly on $\boldsymbol{q}$, we will neglect its presence in the integral except as an upper cut-off for $\boldsymbol{r}_1$ and $\boldsymbol{r}_2$.

Defining the coordinate system of each vector $\boldsymbol{r}_i$ such that $v_{iy} = 0$, we obtain

$$I(\boldsymbol{k}, \epsilon_1, \epsilon_2) = |U|^2 \delta\left(\epsilon - \frac{\boldsymbol{v}\cdot\boldsymbol{v}_1 x_1 + |\boldsymbol{v}\times\boldsymbol{v}_1| y_1}{|\boldsymbol{v}_1|} - \frac{\boldsymbol{v}\cdot\boldsymbol{v}_2 x_2 + |\boldsymbol{v}\times\boldsymbol{v}_2| y_2}{|\boldsymbol{v}_2|}\right)$$
$$= |U|^2 \int \frac{\mathrm{d}y_1\ \mathrm{d}y_2}{|\boldsymbol{v}_1||\boldsymbol{v}_2|}\ \delta\left(\epsilon - \frac{\boldsymbol{v}\cdot\boldsymbol{v}_1\omega_1}{|\boldsymbol{v}_1|^2} - \frac{\boldsymbol{v}\cdot\boldsymbol{v}_2\omega_2}{|\boldsymbol{v}_2|^2} - \frac{|\boldsymbol{v}\times\boldsymbol{v}_1| y_1}{|\boldsymbol{v}_1|} - \frac{|\boldsymbol{v}\times\boldsymbol{v}_2| y_2}{|\boldsymbol{v}_2|}\right). \tag{A2}$$

The main feature of the above result is that the following conditions must be fulfilled for it to be well defined and finite:

(1) $|\boldsymbol{v}_1| \neq 0$;
(2) $|\boldsymbol{v}_2| \neq 0$;
(3) one of the prefactors of y_1 and y_2 in the δ-function must be non-zero.

The last of these conditions means that $\boldsymbol{v} \neq 0$ and that all of the vectors $\boldsymbol{v}$, $\boldsymbol{v}_1$, and $\boldsymbol{v}_2$ cannot be parallel.

We are now in a position to define a set of conditions such that for a scattering process to be dominant, one of them must be met. These conditions are given in equations (5) in the body of the paper, where we also discuss whether these conditions are in fact sufficient for a scattering process to be dominant, and the contribution of each process.

Appendix B. The contribution of a single scattering process to the scattering rate

In this appendix we calculate the contribution of the scattering process given by equation (6*a*) to the function $I(\boldsymbol{k}, \epsilon_1, \epsilon_2)$ defined by equation (4). This contribution will be denoted as $I^s(\boldsymbol{k}, \epsilon_1, \epsilon_2)$. The calculations for each of the two scattering processes described by equations (6*b*) and (6*c*) are identical, except for the different matrix elements which appear in the backward-scattering process. Also, at the end of this appendix we briefly discuss the contribution of other dominant scattering processes, besides those given by equations (6).

We start by making the change of variables $k_{ix}a = q_{ix}$ and $\hbar k_{iy}/\sqrt{4m\Lambda} = q_{iy}$, where $i = 1, 2$. Then, using the energy spectrum given by equation (2), we obtain

$$I^a(\boldsymbol{k}, \epsilon_1, \epsilon_2) = \frac{4m\Lambda}{\hbar^2 a^2} \int \mathrm{d}\boldsymbol{q}_1\ \mathrm{d}\boldsymbol{q}_2\ |U(\boldsymbol{k} - \boldsymbol{k}_1)|^2$$
$$\times\ \delta[\epsilon_1 - 2\Lambda(q_{1y}^2 + 1 - \cos q_{1x})]\delta[\epsilon_2 - 2\Lambda(q_{2y}^2 + 1 - \cos q_{2x})]$$
$$\times\ \delta\big[2\Lambda(q_{1y}^2 + 1 - \cos q_{1x}) + 2\Lambda(q_{2y}^2 + 1 - \cos q_{2x})$$
$$-\ 2\Lambda(q_y^2 + 1 - \cos q_x) - 2\Lambda((q_{1y} + q_{2y} - q_y)^2$$
$$+\ 1 - \cos(q_{1x} + q_{2x} - q_x))\big] \tag{B1}$$

where $\boldsymbol{q}$ is defined with respect to $\boldsymbol{k}$ in the same manner as above. Next, since we are interested in the contribution from the scattering process given by equation (6*a*), we define $x_i \equiv q_{ix} - q_x$, $y_i \equiv q_{iy} - q_y$, and expand in the small variables x_i and y_i, which gives the result

$$I^a(\boldsymbol{k}, \epsilon_1, \epsilon_2) = \frac{m|U(0)|^2}{2\hbar^2 a^2 \Lambda^2} \int_{-\pi}^{\pi} \mathrm{d}x_1\ \mathrm{d}x_2 \int_{-\infty}^{\infty} \mathrm{d}y_1\ \mathrm{d}y_2\ \delta(\omega_1 - 2q_y y_1 - x_1 \sin q_x)$$
$$\times\ \delta(\omega_2 - 2q_y y_2 - x_2 \sin q_x)$$
$$\times\ \delta\left(-2y_1 y_2 - x_1 x_2 \cos q_x + \frac{\sin q_x}{2} x_1 x_2 (x_1 + x_2)\right). \tag{B2}$$

Here $\omega_i \equiv (\epsilon_i - \epsilon_k)/2\Lambda$, and we have kept only leading-order terms in x_i and y_i (except for the cubic term in the last δ-function, which, as we shall see, can be important). After performing the y_1- and y_2-integrals, we obtain

$$I^a(\boldsymbol{k}, \epsilon_1, \epsilon_2) = \frac{m|U(0)|^2}{2\hbar^2 a^2 \Lambda^2} \int_{-\pi}^{\pi} \mathrm{d}x_1 \ \mathrm{d}x_2 \ \delta[2\omega_1\omega_2 - 2\omega_2 x_1 \sin q_x - 2\omega_1 x_2 \sin q_x + (2\sin^2 q_x + 4q_y^2 \cos q_y)x_1 x_2 - 2q_y^2 x_1 x_2 (x_1 + x_2) \sin q_x]. \tag{B3}$$

At this point it is necessary to differentiate between two very different cases, which depend on the value of

$$\kappa(\boldsymbol{q}) = \sin^2 q_x + 2q_y^2 \cos q_y$$

the prefactor of the quadratic term in the δ-function in equation (B3). It is easy to see that this factor is proportional to the curvature of the energy surface at the point $\boldsymbol{k}$, and that if the curvature is zero, then this factor can also be zero. If the prefactor is not small (exact criteria will be given shortly), then the cubic term in the δ-function may be neglected, whereas in the opposite case the cubic term becomes important and the behaviour of the integral is qualitatively changed.

Case 1: $\kappa(\boldsymbol{q})$ is not small. In this case we may neglect the cubic term in the δ-function in equation (B3), and after the appropriate scaling of the variables x_1 and x_2, we obtain

$$I^a(\boldsymbol{k}, \epsilon_1, \epsilon_2) = \frac{m|U(0)|^2}{4\hbar^2 a^2 \Lambda^2 |\kappa(\boldsymbol{q})|} \int_{-\beta_1}^{\beta_1} \mathrm{d}x_1 \int_{-\beta_2}^{\beta_2} \mathrm{d}x_2 \ \delta[\kappa(\boldsymbol{q}) - x_1 \sin q_x - x_2 \sin q_x + x_1 x_2] \tag{B4}$$

where $\beta_i \equiv |\pi\kappa(\boldsymbol{q})/\omega_i|$. The remaining integrations are simple to perform, and yield

$$I^a(\boldsymbol{k}, \epsilon_1, \epsilon_2) = \frac{m|U(0)|^2}{4\hbar^2 a^2 \Lambda^2 |\kappa(\boldsymbol{q})|} \big[\ln|\beta_1 + \sin q_x| + \ln|\beta_1 - \sin q_x| + \ln|\beta_2 + \sin q_x| + \ln|\beta_2 - \sin q_x| - 2\ln|\kappa(\boldsymbol{q}) - \sin^2 q_x|\big]. \tag{B5}$$

If we now use the basic assumption that ω_1 and ω_2 are small parameters, which means that β_1 and β_2 are much bigger than unity, the above expression simplifies to

$$I^a(\boldsymbol{k}, \epsilon_1, \epsilon_2) = \frac{m|U(0)|^2}{2\hbar^2 a^2 \Lambda^2 |\kappa(\boldsymbol{q})|} \big[\ln|\beta_1| + \ln|\beta_2|\big] \tag{B6}$$

This result is given in terms of the original variables in equation (7) of section 3.

Case 2: $\kappa(\boldsymbol{q})$ is small. In this case we may neglect the quadratic term compared to the cubic term in the δ-function in equation (B3). Of the remaining four terms in the δ-function, it is clear that the cubic term is always dominant as long as $x_i > \sqrt{\omega_i}$, which means that the integral diverges as $1/x$. When $x_i \approx \sqrt{\omega_i}$, then the linear terms in the δ-function become important and the divergence is cut off. This means that the main contribution to the integral comes from the region where $x_i \approx \sqrt{\omega_i}$, and therefore that the free term in the δ-function is negligible and the boundaries of integration may be taken to infinity. Using these arguments and scaling the integration variables appropriately, we obtain

$$I^a(\boldsymbol{k}, \epsilon_1, \epsilon_2) = \frac{m|U(0)|^2}{4\hbar^2 a^2 \Lambda^2 |q_y \sin q_x|} \int_{-\infty}^{\infty} \mathrm{d}x_1 \ \mathrm{d}x_2 \ \delta[x_1 - x_2 - x_1 x_2(\omega_2 x_1 + \omega_1 x_2)]. \tag{B7}$$

This double integral can be simplified by going over to polar coordinates, which gives us

$$I^a(\boldsymbol{k}, \epsilon_1, \epsilon_2) = \frac{m|U(0)|^2}{8\hbar^2 a^2 \Lambda^2 |q_y \sin q_x|} \int_0^{2\pi} \mathrm{d}\theta \ \frac{\Theta(-(\sin\theta + \cos\theta)(\omega_2 \sin\theta + \omega_1 \cos\theta))}{\sqrt{-(\sin\theta + \cos\theta)(\omega_2 \sin\theta + \omega_1 \cos\theta)}} \tag{B8}$$

where $\Theta(x)$ is the Heaviside step function. The angular integral can be simplified and the final result is given terms of the original variables by equation (10) in the body of the paper.

We are now in a position to determine the crossover between the above two cases. Referring to equation (B3), and to the discussion in the previous paragraph, it is clear that the crossover occurs when

$$(\sin^2 q_x + 2q_y^2 \cos q_x)x_1x_2 \approx q_y^2(x_1 + x_2)x_1x_2 \sin q_x \qquad \text{and} \qquad x_i \approx \sqrt{\omega_i}.$$

Going back to the original variables, we obtain for the criteria of the crossover region

$$\alpha(\boldsymbol{k}) \approx \epsilon_F\sqrt{\Delta/\Lambda} \tag{B9}$$

where $\alpha(\boldsymbol{k})$ is defined in equation (8).

Finally, we wish to briefly discuss the contribution of other dominant scattering processes, besides those described by equations (6), to the integral $I(\boldsymbol{k}, \epsilon_1, \epsilon_2)$. To do this we use the notation of appendix A and examine a scattering process where $\boldsymbol{k}_i$ is near some arbitrary $\boldsymbol{k}_i^0$ $(i = 1, 2)$. Since the scattering process is dominant, and we are assuming that the Fermi level is far from a saddle point, then condition (5*b*) must hold true. This means that by proceeding in a similar manner to that described by equations (B1)–(B3), one arrives at the result

$$I(\boldsymbol{k}, \epsilon_1, \epsilon_2) = \frac{m|U(0)|^2}{2\hbar^2a^2\Lambda^2}\int_{-\pi}^{\pi} \mathrm{d}x_1\ \mathrm{d}x_2\ \delta\big[a\epsilon + b\epsilon x_1 + c\epsilon x_2 + dx_1^2 + ex_2^2 + fx_1x_2 + (\text{third-order terms})\big]. \tag{B10}$$

Here $\epsilon \equiv \Delta/\Lambda$ and a, b, c, d, e, and f are all dimensionless parameters that depend on $\boldsymbol{k}$, $\boldsymbol{k}_1^0$, and $\boldsymbol{k}_2^0$, and are generally of the order of ϵ_F/Λ. The result is arrived at by employing condition (5*b*) so that all linear terms in the δ-function that are not proportional to ϵ vanish. It can be seen from equation (B10) that

$$I(\boldsymbol{k}, \epsilon_1, \epsilon_2) \approx \frac{m|U(0)|^2}{2\hbar^2a^2\Lambda\epsilon_F}\ln\left[\frac{\epsilon_F}{\Delta}\right] \tag{B11}$$

and hence that the contribution of the scattering process to $I(\boldsymbol{k}, \epsilon_1, \epsilon_2)$ is of the same order as the contribution of the scattering processes given by equations (6). Note that the case in which $\boldsymbol{k}$ is near a zero-curvature point is not relevant to the current discussion, since then only the scattering processes given by equations (6) can be dominant (figure 1(b)).

References

[1] Messica A, Soibel A, Meirav U, Stern A, Shtrikman H, Umansky V and Mahalu D 1997 *Phys. Rev. Lett.* **78** 705
[2] Soibel A, Meirav U, Mahalu D and Shtrikman H 1997 *Phys. Rev.* B **55** 4482
[3] Kardynal B, Barnes C H W, Linfield E H, Ritchie D A, Brown K M, Jones G A C and Pepper M 1996 *Phys. Rev. Lett.* **76** 3802
[4] Beenakker C W J 1989 *Phys. Rev. Lett.* **62** 2020
[5] Gerhardts R R, Weiss D and von Klitzing K 1989 *Phys. Rev. Lett.* **62** 1173
[6] Winkler R W, Kotthaus J P and Ploog K 1989 *Phys. Rev. Lett.* **62** 1177
[7] Umansky V, de Picciotto R and Heiblum M 1997 *Appl. Phys. Lett.* **71** 683
[8] Reich K K, Ferry D K, Grondin R O and Iafrate G J 1982 *Phys. Lett.* **91A** 28
[9] Kelly M J 1984 *J. Phys. C: Solid State Phys.* **17** 781
[10] Das A K, Glasser M L and Payne S H 1988 *J. Phys. C: Solid State Phys.* **21** 357
[11] Murphy S Q, Eisenstein J P, Pfeiffer L N and West K W 1995 *Phys. Rev.* B **52** 14 825
[12] Lee P and Ramakrishnan T V 1985 *Rev. Mod. Phys.* **57** 287
[13] Fukuyama H and Abrahams E 1983 *Phys. Rev.* B **27** 5976
[14] Gopalan S, Gunnarsson O and Andersen O K 1992 *Phys. Rev.* B **46** 11 798

[15] Pattnaik P C, Kane C L, Newns D M and Tsuei C C 1992 *Phys. Rev.* B **45** 5714
[16] Newns D M, Tsuei C C, Huebener R P, van Bentum P J M, Pattnaik P C and Chi C C 1994 *Phys. Rev. Lett.* **73** 1695
[17] Yacoby A, Sivan U, Umbach C P and Hong J M 1991 *Phys. Rev. Lett.* **66** 1938
Yacoby A, Heiblum M, Shtrikman H, Umansky V and Mahalu D 1994 *Semicond. Sci. Technol.* **9** 907
[18] Zheng L and Das Sarma S 1996 *Phys. Rev.* B **53** 9964
[19] Lu J P and Shayegan M 1996 *Phys. Rev.* B **53** R4217
[20] Menashe D and Laikhtman B 1996 *Phys. Rev.* B **54** 11 561
[21] Chaplik A V 1971 *Zh. Eksp. Teor. Fiz.* B **60** 1845 (Engl. Transl. 1971 *Sov. Phys.–JETP* **33** 997)
[22] Guiliani G F and Quin J J 1982 *Phys. Rev.* B **26** 4421
[23] Fukuyama H and Ogata M 1994 *J. Phys. Soc. Japan* **63** 3923